J Petrol Explor Prod Technol (2017) 7:1197–1203
DOI 10.1007/s13202-016-0306-y

CrossMark

SHORT COMMUNICATION - PRODUCTION ENGINEERING

A theory-based simple extension of Peng–Robinson equation of state for nanopore confined fluids

Akand W. Islam[1] · Alexander Y. Sun[2]

Received: 9 October 2016 / Accepted: 27 November 2016 / Published online: 19 December 2016

Abstract In a recent publication (Islam et al. in J Nat Gas Sci Eng 25:134–139, 2015), the van der Waals equation of state (EOS) was modified to assess phase behavior of nanopore confined fluids. Although the changes of critical properties were well captured, it was limited to only sub-critical conditions. Peng–Robinson EOS showed inconsistent critical shifts. Here, we develop a simple extension of Peng–Robinson (PR) derived similarly from the Helmholtz free energy function by applying the same energy and volume parameter relations. This modified PR reproduces experimental and molecular simulation results satisfactorily. It shows that there is pore proximity effect also in supercritical condition which, however, diminishes as temperature increases. The proposed model can show heterogeneous density or layered distribution of molecules inside nanopore. We have tested common shale (natural) gas molecules and the condition of Haynesville plays where temperature and pressure can be very high. This simple model can offer alternatives to more computationally expensive molecular simulations to study the pore proximity phenomenon.

Keywords Proximity effect · Capillary condensation · Nanopore · Tight shale reservoir · PVT behavior · Reservoir simulation

List of symbols

A Pore cross-sectional area (dm^2)
d Diameter (dm)
F Helmholtz free energy ($mol/dm/s^2$)
k Boltzman constant
N Avogadro number
P Pressure (MPa)
r Radius (dm) ($d = 2r$)
$\wp$ Radial distance (dm)
ρ Density (mol/dm^3)
R Universal gas constant (dm^3 MPa/mol/K)
s Intermolecular distance (dm)
T Temperature (K)
$\bar{V}$ Specific volume (dm^3/mol)
V Pore volume (dm^3)

Greek symbol

σ Lennard-Jones size parameter (Å)
ε Lennard-Jones energy parameter (dm/s^2)

Subscripts

1, 2 Molecules id's
b Bulk
c Critical
x Axial direction
p Pore
r Reduced parameter

✉ Akand W. Islam
wahid807@gmail.com

1 12398 Risman Dr., Plymouth, MI, USA

2 Bureau of Economic Geology, The University of Texas at Austin, Austin, TX, USA

Introduction

The confinement in geologic formations can introduce important effects on many physical properties of fluids entrapped inside the pores, including the phase equilibria (Tan and Piri 2015; Sing and Williams 2012). Phase transitions such as capillary condensation occur due to pore proximity at temperatures and pressures different than in the bulk. The introduction of wall forces, and the competition between fluid–wall and fluid–fluid forces, can lead to irregularities, such as layering, wetting and commensurate–incommensurate transitions, shifts in freezing, liquid–liquid equilibrium, and other common bulk thermodynamic behaviors (Gelb et al. 1999). Actually when the pore size becomes comparable to the intermolecular separations, a large fraction of confined molecules experiences a reduction in the number of nearest-neighbor molecules, and this hetero-distributions lead to shifting of phase coexistence curve and lowering of critical points. This kind of phenomenon is well established, and a good number of physical models, covering from the Kelvin equation (Mitropoulos 2008; Powles 1985; Shapiro and Stenby 1997; Thompson 1871) to those based on the density functional theory (Gelb et al. 1999; Evans et al. 1986; Li et al. 2014; Tarazona et al. 1987; Ustinov and Do 2005; Wu 2006), are proposed. The formers have been applied to practical applications in a wide range of disciplines. The latter models, however, are generally intended for simulation and theoretical investigation of the confined fluids, due to their intensive mathematical and computational frameworks. The theories have contributed plausible explanation to the underlying mechanisms that are mostly inaccessible to experimental validation at this time, including their implication as a reliable way for estimating pore radii (Tan and Piri 2015; Neimark and Ravikovitch 2001). There are cubic EOS models available to quantify confinement effects through capillary pressure modifications (Ghasemi et al. 2014; Gildin et al. 2013; Yan et al. 2013; Alfi et al. 2016a, b). In these cases, it is assumed that adsorption of confined fluids depends on different factors such as molecular structure of the pore wall surface, the polarization and size of molecules, and their interaction with the solid. These models show the relation between amounts of fluid adsorbed on the solid surface and the system temperature/pressure. The Langmuir type isotherms are particularly used to predict adsorption. The Young–Laplace equation is applied to compute capillary pressure.

The phase behavior of confined fluids has many practical applications, such as separation processes, oil extraction, estimation of gas-in-place and reserves, heterogeneous catalysis, molecular transport, among others (Didar and Akkutlu 2013; Holt et al. 2006; Pitabunkate et al. 2014; Travalloni et al. 2010). Over the past decades, one of the major focuses of petroleum industries has been to develop shale gas exploration technology. Unlike conventional sandstone and carbonate reservoirs, shale plays have unique rock properties and, in particular, ultra-low in situ permeabilities on the order of 1–100 nanodarcy (Pitabunkate et al. 2014). The shale reservoirs contain extremely tight nanopores, leading to the ultra-low permeabilities. It is nearly impossible to extract hydrocarbon fluids from shale reservoirs without substantial stimulation of the formation, and the currently favored model is that of the multi-fractured horizontal well. The ultra-low permeabilities, combined with the requirement of substantial stimulation to achieve commercial flow rates, have led to the descriptor of "unconventional reservoirs" for shale plays (Pitabunkate et al. 2014; Islam and Patzek 2014; Passey et al. 2010; Shabro et al. 2011). The EOS derived for bulk fluid (e.g., Redlich and Kwong 1949; Peng and Robinson 1976) is not appropriate for phase equilibrium calculations of the tight shale reservoirs. On the other hand, van der Waals modified for nanopores (e.g., Zarragoicoechea and Kuz 2002; Islam et al. 2015) is not a good candidate for bulk phase estimations. Hence to bridge this gap, our motivation is to deduce an EOS for both tight shale reservoirs and conventional $P\bar{V}T$ simulations. We select PR, a popular choice of petroleum industries, for modification. Travalloni et al. (2014) recently have presented an extension of PR to this end by introducing confinement modified attractive terms. They showed non-differentiable axial and radial components of the pressure, as a uniform quantity. We present here different forms, applicable for general purpose tight shale reservoir simulations. In addition, we aim to show property changes in supercritical condition.

Model

Reduction in the size of a cylindrical pore leads to one dimensional behavior. Hence, investigation of confined fluids' behavior in such tight pore provides a way to study the size effects (Gelb et al. 1999). We aim to observe only changes of state conditions ($P\bar{V}T$). The variables such as molecular structure of the pore surface and connectivity are ignored. We assume only vapor–liquid equilibria, or capillary condensation/evaporation exists. The wall forces, the competition between fluid and wall, and other forms of phase transitions (e.g., liquid–liquid equilibria, freezing) are ignored.

The modified van der Waals EOS (Islam et al. 2015) deduced from the Helmholtz free energy function of a system of N particles interacting by a pair potential $U(s_{12})$ reads as

$$F = f(T) - \frac{kTN^2}{2V^2}\int\int\left(e^{-\frac{U(s_{12})}{kT}} - 1\right)dV_1 dV_2, \quad (1)$$

where $f(T)$ is the free energy of ideal gas. After derivations, we obtained F expressed below.

$$F = f(T) + \frac{kTN^2}{V}b + \frac{kTN^2}{2V^2}\int\int_{s_{12}>\sigma}\frac{U(s_{12})}{kT}dV_1 dV_2 \quad (2)$$

The integral was solved for $s_{12} > \sigma$, numerically. We obtained approximation of the double integral in Eq. (2) as

$$\frac{1}{V}\int_{s_{12}>\sigma}\int \frac{U(s_{12})}{kT}\mathrm{d}V_1\mathrm{d}V_2 = \frac{4\varepsilon}{kT}\sigma^3 f\left(\frac{d_\mathrm{p}}{\sigma}\right). \tag{3}$$

Here $f\left(\frac{d_\mathrm{p}}{\sigma}\right) = \left[c_0 + c_1/\frac{d_\mathrm{p}}{\sigma} + c_2/\left(\frac{d_\mathrm{p}}{\sigma}\right)^2\right]$. The predicted values after reduction were $c_0 = -2.7925$, $c_1 = 2.6275$, and $c_2 = -0.6743$. The numerical values of Eq. (3) and the fitting curve of $f\left(\frac{d_\mathrm{p}}{\sigma}\right)$ are presented in Fig. 1. It turns out that the pore diameter equivalent to 100 molecules size can be considered as the cutoff or critical size of proximity below which metastability rises. The metastability refers to the redundancy of intramolecular bulk equilibrium state where their interactions become singular and continuous phase transitions disappear. The $P\bar{V}T$ relations in this case are a very strong function of pore size.

After differentiating as $P_x = -\frac{1}{L_z}\frac{\partial F}{\partial A_\mathrm{p}}\Big|_{T,L_z}$ and $P_z = -\frac{1}{A_\mathrm{p}}\frac{\partial F}{\partial L_z}\Big|_{T,A_\mathrm{p}}$, where $A_\mathrm{p} = \pi\left(\frac{r_\mathrm{p}}{\sigma}\right)^2$, the equivalent radial and axial pressures of PR are

$$P_\mathrm{r} = \frac{RT}{\bar{V}-b} - \frac{a - \sigma^3\varepsilon N^2\frac{\sigma}{r_\mathrm{p}}\left(3c_1 + 4c_2\frac{\sigma}{r_\mathrm{p}}\right)}{\bar{V}(\bar{V}+b) + b(\bar{V}-b)}, \tag{4}$$

$$P_x = \frac{RT}{\bar{V}-b} - \frac{a - 2\sigma^3\varepsilon N^2\frac{\sigma}{r_\mathrm{p}}\left(c_1 + c_2\frac{\sigma}{r_\mathrm{p}}\right)}{\bar{V}(\bar{V}+b) + b(\bar{V}-b)}. \tag{5}$$

The expressions of PR presented by Eqs. (4) and (5) were obtained previously (Islam et al. 2015). They failed to exhibit any size effect. Henceforth, we term them as the original PR for comparisons with the new equations proposed in subsequent discussion.

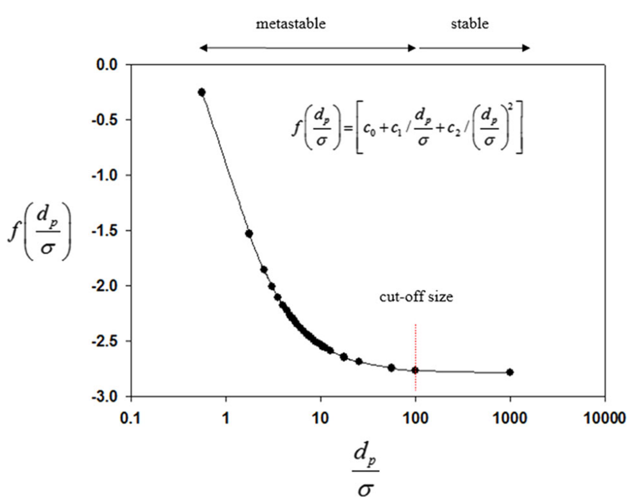

Fig. 1 Interaction energy function with respect to $\frac{d_\mathrm{p}}{\sigma}$. The *circles* represent numeric values of double integral of Eq. 3, and the *line* shows corresponding quadratic fit

For modification, the perturbation term is extended. As mentioned, when $\frac{\sigma}{r_\mathrm{p}} \le 0.01$, the proximity effect tends to be important. The effect is maximum when $\frac{\sigma}{r_\mathrm{p}} \approx 1.25$. The perturbation term is

$$\bar{V}(\bar{V}+b) + b(\bar{V}-b) \approx \bar{V}^2 + k_1 + \frac{k_2}{\frac{\sigma}{r_\mathrm{p}}}. \tag{6}$$

We have predicted k_1 and k_2 by solving two cases of $\frac{\sigma}{r_\mathrm{p}}$ below, which are chosen considering extreme tight pore and near bulk conditions,

$$\frac{\sigma}{r_\mathrm{p}} = 1.25 \Rightarrow k_1 + \frac{k_2}{\frac{\sigma}{r_\mathrm{p}}} = 0 \tag{7}$$

$$\frac{\sigma}{r_\mathrm{p}} = 0.01 \Rightarrow k_1 + \frac{k_2}{\frac{\sigma}{r_\mathrm{p}}} = b(2\bar{V} - b) \tag{8}$$

From Eqs. (7) and (8), the values obtained are $k_1 = 0.0081\,(b^2 - 2\bar{V}b)$ and $k_2 = 0.0101\,(2\bar{V}b - b^2)$. When $\frac{\sigma}{r_\mathrm{p}} \ge 0.01$, the bulk phase (Peng and Robinson 1976) is retained. The volume and energy terms are correlated as

$$a' = \Omega_{a,\mathrm{p}}\Omega_a\frac{R^2T_\mathrm{c}^2}{P_\mathrm{c}}, \tag{9}$$

$$b' = \Omega_{\mathrm{b,p}}\Omega_\mathrm{b}\frac{RT_\mathrm{c}}{P_\mathrm{c}}. \tag{10}$$

Here $\Omega_{a,\mathrm{p}}$ and $\Omega_{\mathrm{b,p}}$ are predicted by data reduction of critical shifts compiled in Islam et al. (2015); Ω_a and Ω_b are obtained from the standard PR EOS (Peng and Robinson 1976). Table 1 reports the values.

The final expressions of PR can be written as

$$P_\mathrm{r} = \frac{RT}{\bar{V}-b'} - \frac{a' - \sigma^3\varepsilon N^2\frac{\sigma}{r_\mathrm{p}}\left(3c_1 + 4c_2\frac{\sigma}{r_\mathrm{p}}\right)}{\bar{V}^2 + k_1 + \frac{k_2}{\frac{\sigma}{r_\mathrm{p}}}}, \tag{11}$$

$$P_x = \frac{RT}{\bar{V}-b'} - \frac{a' - 2\sigma^3\varepsilon N^2\frac{\sigma}{r_\mathrm{p}}\left(c_1 + c_2\frac{\sigma}{r_\mathrm{p}}\right)}{\bar{V}^2 + k_1 + \frac{k_2}{\frac{\sigma}{r_\mathrm{p}}}}, \tag{12}$$

and the effective global pressure $P_\mathrm{eff} = \frac{1}{2}(P_x + P_\mathrm{r})$. It is noteworthy that the proposed model is targeted for single component only. In our future development, we will aim to model multicomponent mixtures.

Results and discussion

This new extended PR exhibits phase changes of fluids with squeezing pore sizes. The equation shows existence of VLE of CH_4 through Maxwell construction as seen in Fig. 2 at $\frac{\sigma}{r_\mathrm{p}} = 0.18$, $T_\mathrm{r} = 0.75$. However, the original PR shows the supercritical state. The reduced temperature is

Table 1 Parameters of PR EOS

$\frac{\sigma}{r_p} \leq 0.01$		$\frac{\sigma}{r_p} > 0.01$	
$\Omega_{a,p}$	0.77367	$\Omega_{a,p}$	1.0
Ω_a	0.45724	Ω_a	0.45724
$\Omega_{b,p}$	0.6652	$\Omega_{b,p}$	1.0
Ω_b	0.321	Ω_b	0.321

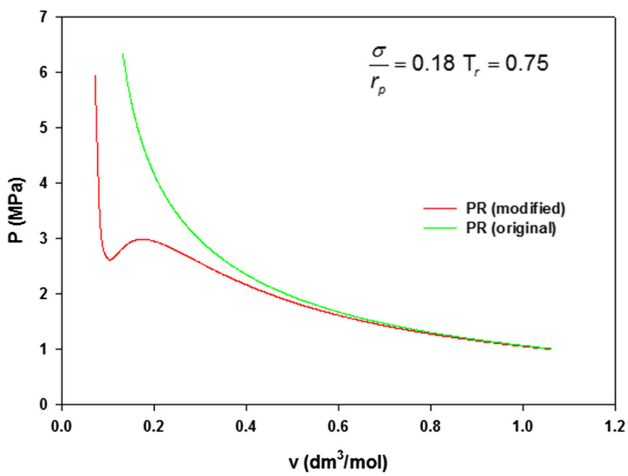

Fig. 2 Phase change of CH_4 shown by modified PR

defined as $T_r = \frac{T}{T_{c,b}}$. $T_{c,b}$ is the bulk phase critical temperature.

It is evident that unlike in the bulk phase, radial and axial pressures are different due to pore proximity. Because motions of molecules become restricted, radial pressure increases more than that in the axial direction. At the pore wall ($\wp = r_p$), a first-order phase transition accompanied by an infinitely sharp change in a suitable order parameter, usually the density or composition, is experienced. The proposed PR captures this phenomenon well, as can be seen in Fig. 3 for CH_4. The effect is more acute in low temperatures (subcritical). Figure 4 shows results of $T_r = 0.75$. The confined molecules can separate into layers posing equal free energies (Gelb et al. 1999). Molecular simulations display this behavior as the heterogeneous distribution of molecules within the slit plates (see Severson and Snurr 2007; Singh et al. 2009; Harrison et al. 2014). By using our model, we can see from Fig. 5 how density profiles vary from the center to pore wall, indicating damped oscillation of the trapped molecules. The results are shown of 5 nm pore size in both low and high temperatures and pressures. They are consistent with the molecular simulations investigated in (Didar and Akkutlu 2013; Diaz-Campos 2010). Our calculations match quantitatively well. For instance, at 355 K and 27.5 MPa in 3.05 nm pore width, the obtained density of CH_4 from Didar and Akkutlu (2013) at 1.14 nm

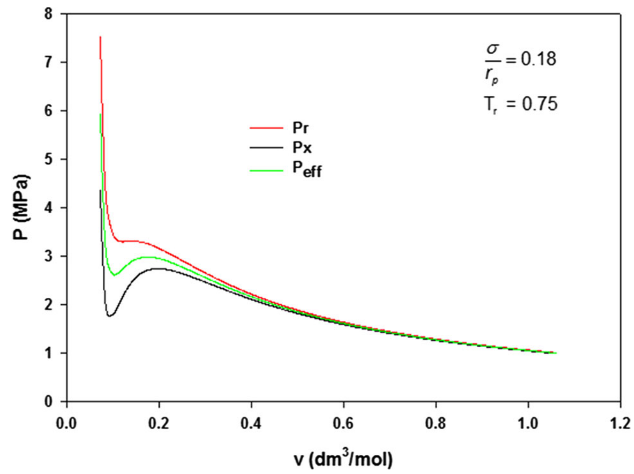

Fig. 3 Radial and axial pressures of CH_4 calculated by proposed PR

apart from center is ~8000 mol/m3, while model predicted value is 7990 mol/m^3.

There are three characteristics regions of the density distribution: the adsorbed layer which is the closest to the wall and the most impacted, the phase transition layer across which a significant change of density is observed, and the central layer which in this case is the quasi-bulk phase. In some cases, temperature and pressure of shale reservoirs can be very high. Figure 5b presents the condition of Haynesville plays, which is very deep (10,000 ft), and temperature and pressure can reach to 450 K and 80 MPa, respectively (Male et al. 2015). As expected, at higher temperature and pressure, relative change of volumetric property is less. Figure 6 shows how density of CH_4 changes from nearly bulk phase ($\frac{\sigma}{r_p} = 0.01$) to extreme tight condition ($\frac{\sigma}{r_p} = 1.25$). Temperature shows clear effect on the isotherm. Severson and Snurr (2007) studied pentane isotherms ranging from 300 to 1500 K. They found that at any given pressure the density decreases as the temperature increases. The effect is less at higher temperatures, although not diminishes completely. The distribution of molecules is less heterogeneous throughout the pore volume.

Figure 7 shows critical temperature change to 154.8 K from 190.6 K at $\frac{\sigma}{r_p} = 0.18$. The critical properties can be computed from this modified PR either graphically or by solving the equations $\frac{\partial P}{\partial V}\Big|_T = \frac{\partial^2 P}{\partial V^2}\Big|_T = 0$ iteratively. The critical properties data are consistent with the molecular simulation results reported in (Didar and Akkutlu 2013; Singh et al. 2009; Ortiz et al. 2005; Vishnyakov et al. 2001). Islam et al. (2015) presented data compilation of critical temperature and pressure changes. We have also tested calculations of N_2. Figure 8 shows results of axial, radial, and effective pressures of N_2.

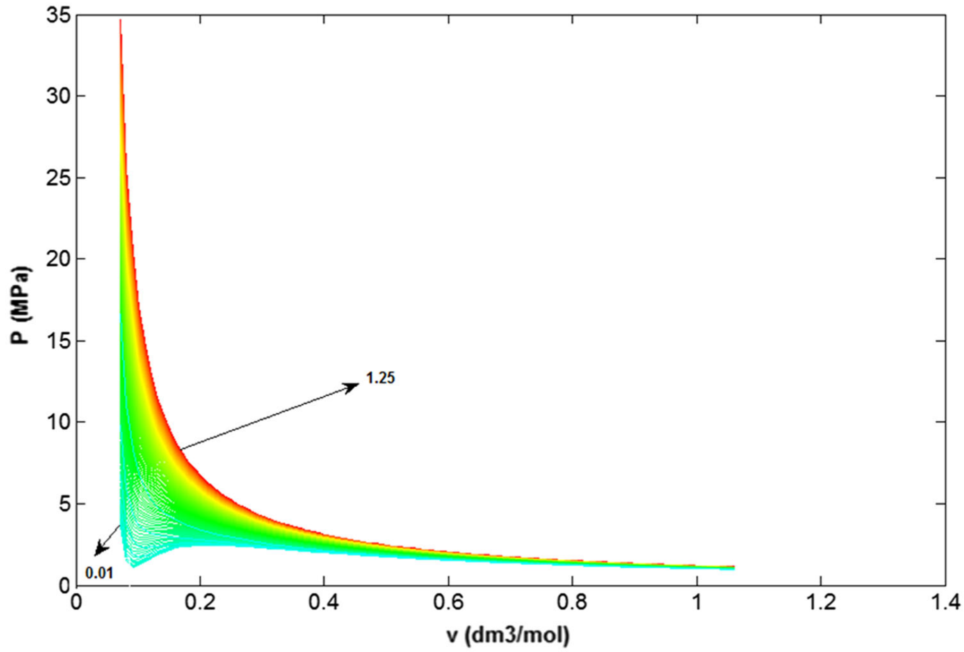

Fig. 4 Density changes of CH_4 at $T_r = 0.75$. Results show 125 graphs with step size of 0.01 starting from $\frac{\sigma}{r_p} = 1.25$–0.01

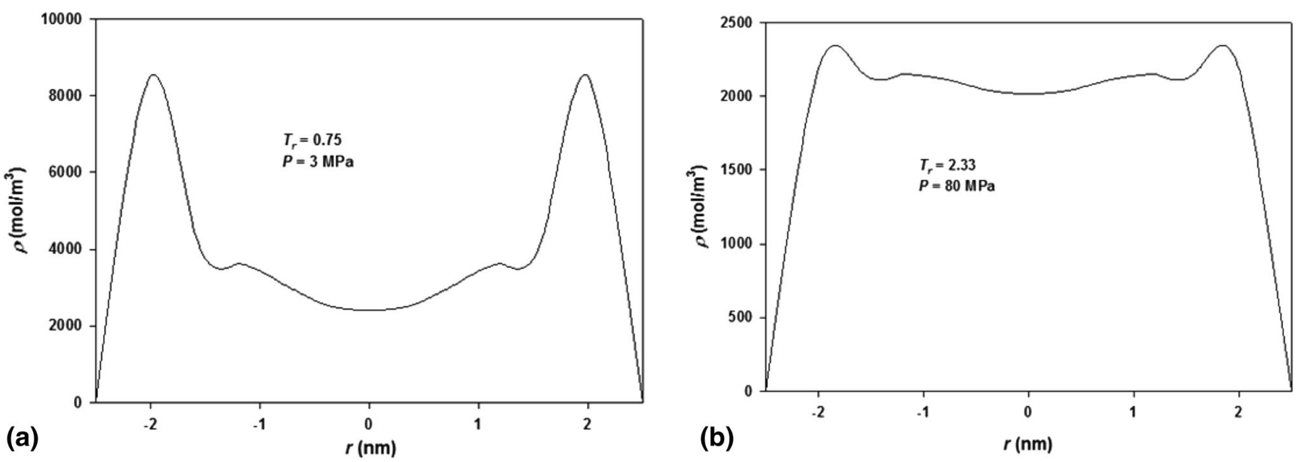

Fig. 5 Heterogeneous (layered) density profiles of CH_4 inside the pore

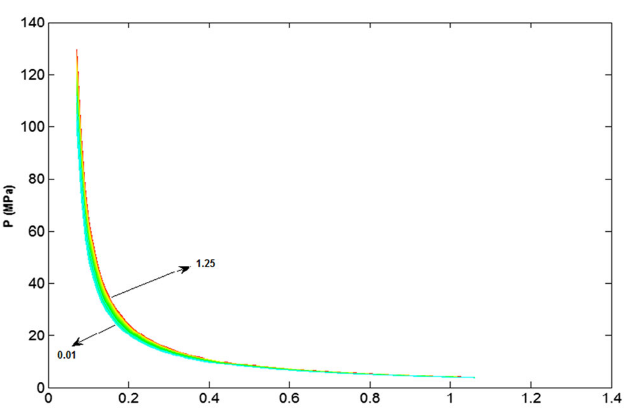

Fig. 6 Density changes of CH_4 at $T_r = 2.5$. Results show 125 graphs with step size of 0.01 starting from $\frac{\sigma}{r_p} = 1.25$–0.01

In petroleum industries, PR is widely used for simulating volumetric properties of natural or shale gas in reservoir simulations. The major advantage of this modification is that Eqs. (10) and (11) can be applied to both tight pores and bulk phase conditions. When $\frac{\sigma}{r_p} > 0.01$, the size contribution disappears. Figures 9 and 10 show critical property changes of C_4H_{10} and CO_2. They are also consistent with the trend of critical shifts as we have observed for CH_4 and N_2.

Concluding remarks

There have been considerable advances in our understanding of phase equilibria and separation in nanopores; however, theoretical presentation through a simple EOS is

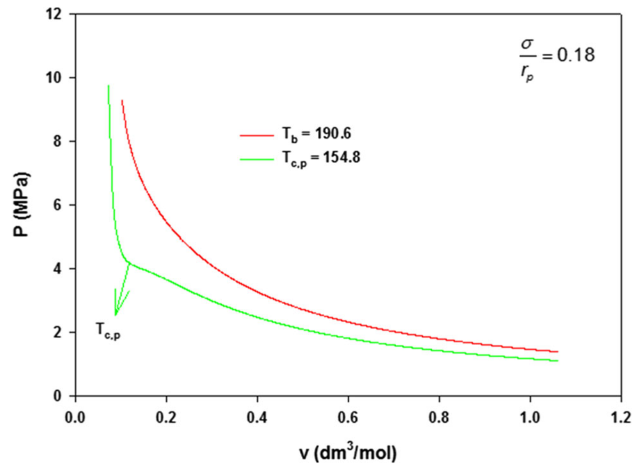

Fig. 7 Representation of critical temperature and pressure of CH_4 changed from bulk phase at $\frac{\sigma}{r_p} = 0.18$

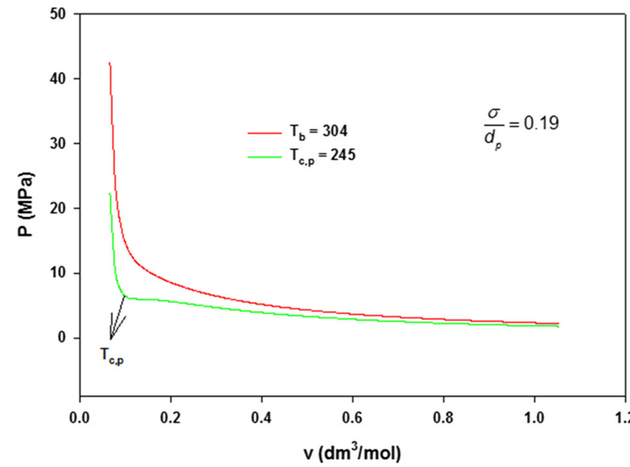

Fig. 10 Representation of critical temperature and pressure of CO_2 changed from bulk phase

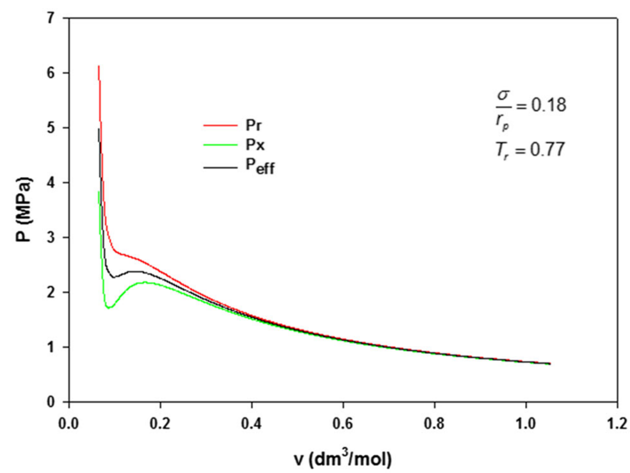

Fig. 8 Radial, axial, and effective pressures of N_2

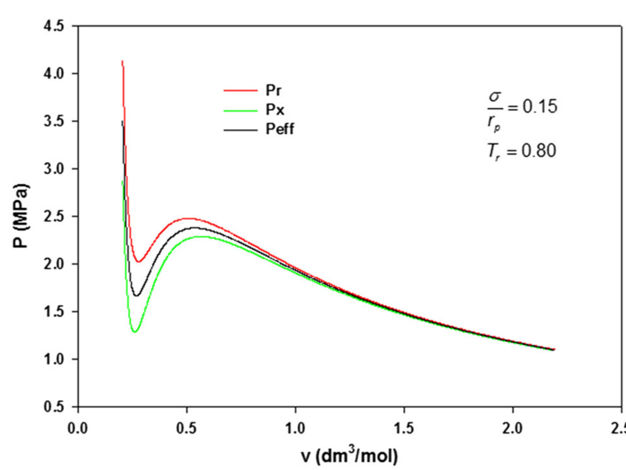

Fig. 9 Radial, axial, and effective pressures of C_4H_{10}

still lacking. The extended PR proposed here incorporates the proximity effects satisfactorily, both in subcritical and supercritical conditions. This simple model limits the gap between bulk phase and nanopore thermodynamic for a wide range of temperature and pressure. Because our model shows transition from nanopore to bulk state phase equilibria, it can simultaneously be used for conventional $P\bar{V}T$ calculations as well as for tight shale reservoir simulations. Compared to the molecular simulations, the model exhibits heterogeneous or layered density profiles across the nanopore satisfactorily.

Acknowledgements The authors are thankful to Prof. Tad Patzek of King Abdullah University of Science and Technology and Prof. John Pausnitz of University of California at Berkeley for their suggestions in developing the model. The authors greatly acknowledge the anonymous reviewer for constructive comments.

References

Alfi M, Yan B, Cao Y, An C, Killough J, Barrufet M (2016a) Microscale porosity models as powerful tools to analyze hydrocarbon production mechanisms in liquid shale. J Nat Gas Sci Eng 26:1495–1505

Alfi M, Nasrabadi H, Banerjee D (2016b) Experimental investigation of confinement effect on phase behavior of hexane, heptane and octane using lab-on-chip technology. Fluid Phase Equilib 423:25–33

Diaz-Campos M (2010) Uncertainities in shale gas—in place calculations. University of Oklahoma, Norman

Didar BR, Akkutlu Y (2013) Pore-size dependence of fluid phase behavior and properties in organic-rich shale reservoirs. In: SPE international symposium on oilfield chemistry. The Woodslands, 8–10 Apr 2013

Evans R, Marconi U, Tarazona P (1986) Capillary condensation and adsorption in cylindrical and slit-like pores. J Chem Soc Faraday Trans 82:1763–1787

Gelb L, Gubbins K, Radhakrishnan R, Sliwinska-Bartkowiak M (1999) Phase separation in confined systems. Rep Prog Phys 62:1573–1659

Ghasemi M, Ibrahim A, Gildin E (**2014**) Reduced order modeling in reservoir simulation using the bilinear approximation techniques. In: SPE Latin America and Caribbean petroleum engineering conference. Society of Petroleum Engineers, Maracaibo

Gildin E, Ghasemi M, Romanovskay A, Efendiev Y (2013) Nonlinear complexity reduction for fast simulation of flow in heterogeneous porous media. In: SPE reservoir simulation symposium. Society of Petroleum Engineers, Woodlands

Harrison A, Cracknell R, Kruger-Venus J, Sarkisov L (2014) Branched versus linear alkane adsorption in carbonaceous slit pores. Adsorption 20:427–437

Holt JK, Park HG, Wabg Y, Stadermann M, Artyukhin AB, Grigoropoulos CP, Noy A, Bakajin O (2006) Fast mass transport through sub-2-nanometer carbon nanotubes. Science 312:1034–1037

Islam A, Patzek T (2014) Slip in natural gas flow through nanoporous shale reservoirs. J Unconv Oil Gas Res 7:49–54

Islam A, Patzek T, Sun A (2015) Thermodynamics phase changes of nanopore fluids. J Nat Gas Sci Eng 25:134–139

Li Z, Jin Z, Firoozabadi A (2014) Phase behavior and adsorption of pure substances and mixtures and characterization in nanopore structures by density functional theory. SPE J 19:1096–1109

Male F, Islam A, Patzek T, Ikonnikova S, Browning J, Marder M (2015) Analysis of gas production from hydraulically fractured wells in the Haynesville Shale using scaling methods. J Unconv Oil Gas Res 10:11–17

Mitropoulos A (2008) The Kelvin equation. J Colloid Interface Sci 317:643–648

Neimark A, Ravikovitch P (2001) Capillary condensation in MMS and pore structure characterization. Microporous Microporous Mater 44:697–707

Ortiz V, Lopez-Alvarez YM, Lopez GE (2005) Phase diagrams and capillary condensation of confined in single- and multi-layer nanotube. Mol Phys 103:2587–2592

Passey R, Bohacs M, Esch L, Klimenditis R, Sinha S (2010) From oil-prone source rock to gas-producing shale reservoir-geologic and petrophysical characterization of unconventional shale gas reservoirs. In: International oil and gas conference and exhibition. Beijing, 8–10 June 2010

Peng D-Y, Robinson DB (1976) A new two-constant equation of state. Ind Eng Chem Fundam 15:59–64

Pitabunkate T, Balbuena P, Moridis G, Blasingame T (2014) Effect of confinement on PVT properties of hydrocarbons in shale reservoirs. In: SPE ATCE. Amsterdam 27–29 Oct 2014

Powles J (1985) On the validity of the Kelvin equation. J Phys A: Math Gen 18:1551–1560

Redlich O, Kwong JNS (1949) On the thermodynamics of solutions. Chem Rev 44:233–244

Severson BL, Snurr RQ (2007) Monte Carlo simulation of *n*-alkane adsorption isotherms in carbon slit pores. J Chem Phys 126:134708

Shabro V, Torres-Verdin C, Javadpour F (2011) Numerical simulation of shale-gas production: from pore-scale modeling of slip-flow, Knudsen diffusion, and langmuir desorption to reservoir modeling of compressible fluid. In: SPE North American unconventional gas conference and exhibition. Woodlands, 14–16 June 2011

Shapiro A, Stenby E (1997) Kelvin equation for a non-ideal multicomponent mixture. Fluid Phase Equilib 134:87–101

Sing K, Williams R (2012) Historical aspects of capillarity and capillary condensation. Microporous Microporous Mater 154:16–18

Singh SK, Sinha A, Deo G, Singh J (2009) Vapor-liquid phase coexistence, critical properties, and surface tension of confined alkanes. J Phys Chem 113:7170–7180

Tan S, Piri M (2015) Equation-of-state modeling of confined-fluid phase equilibria in nanopores. Fluid Phase Equilib 393:48–63

Tarazona P, Marconi U, Evans R (1987) Phase equilibria of fluid interfaces and confined fluids. Non-local versus local density functionals. Mol Phys 60:573–595

Thompson W (1871) On the equilibrium of vapour at a curved surface of liquid. Philos Mag 42:448–452

Travalloni L, Castier M, Tavares FW, Sandler SI (2010) Thermodynamic modeling of confined fluids using an extension of the generalised van der Waals theory. Chem Eng Sci 65:3088–3099

Travalloni L, Castier M, Tavares F (2014) Phase equilibrium of fluids confined in porous media from an extended Peng–Robinson equation of state. Fluid Phase Equilib 362:335–341

Ustinov E, Do D (2005) Modeling of adsorption in finite cylindrical pores by means of density functional theory. Adsorption 11:455–477

Vishnyakov A, Piotrovskaya EM, Brodskaya EN, Votyakov EV, Tovbin YK (2001) Critical properties of Lennard-Jones fluids in narrow slit pores. Langmuir 17:4451–4458

Wu J (2006) Density functional theory for chemical engineering; from capillary to soft materials. AIChE J 52:1169–1193

Yan B, Alfi M, Wang Y, Killough J (2013) A new approach for the simulation of fluid flow in unconventional reservoirs through multiple permeability modeling. In: SPE annual technical conference and exhibition. Society of Petroleum Engineers, New Orleans

Zarragoicoechea GJ, Kuz VA (2002) van der Waals equation of state for a fluid in a nanopore. Phys Rev E 65:021110